

# UHF Wideband Mobile Channel Measurements and Characterization using ATSC Signals with Diversity Antennas

Assia Semmar, Viet Ha Pham, Jean-Yves Chouinard  
Department of Electrical and Computer Engineering  
Laval University, Québec, Qc, Canada G1K-7P4  
email: {assia,phamviet,chouinar}@gel.ulaval.ca.

Sébastien Laffèche, Xianbin Wang, Yiyan Wu  
Communications Research Centre Canada  
3701 Carling Ave., Ottawa, Ontario, Canada, K2H 8S2  
email: {sebastien.lafleche, xianbin.wang, yiyan.wu}@crc.ca.

## Abstract:

Recently, there have been increasing interests to characterize the UHF wideband mobile reception. In the literature, there are several studies on UHF mobile reception for cellular phone systems, however, most of them addresses narrowband services. This paper presents propagation measurement results on UHF TV band using the ATSC Digital Television as a sounding signal to study the characteristics of wideband Digital Television (DTV) channel under mobile reception conditions. The analysis of the measurement data presented in this paper shows that channel characteristics depend strongly on surrounding environments and receiver's parameters, such as the vehicle speed relative to the transmitter-receiver axis.

**Index Terms-** terrestrial digital television, wideband channel characterization and modeling, mobile reception, antenna diversity.

## I. INTRODUCTION

The digital terrestrial television standard, ATSC 8-VSB, adopted by the Federal Communications Commission [1] in December 1996 is designated to stationary reception of video services. But since then, where there is already a high penetration of cable and satellite reception, mobile and portable reception have been identified as a unique selling point for digital terrestrial television. The development of such services requires a good knowledge of the channel characteristics and their statistical parameters which are of great importance in the design of all parts of the system and planning of radio systems.

In this paper, we present the recent results of a measurement campaign conducted to characterize the digital terrestrial television propagation channel for mobile applications in the area of Ottawa, Canada. The data is analyzed to provide statistical parameters of the UHF DTV channel. The method used in this work allows us to extract the channel impulse response directly from measured data. From those channel impulses responses, we derive some useful correlations and power spectral density functions that define the characteristics of a fading multipath channel. The main problems associated with mobile reception of broadcast signals are the Doppler effects and the multipath fading caused by reflection and scattering from obstructions in the vicinity of the receiver. Antenna diversity is an effective way to decrease the effect of multipath fading. The mobile was equipped with two antennas for spatial diversity. The signals obtained from the two antennas may be combined by selection

combining, equal-gain combining or maximal-ratio combining to improve the quality of the system.

The outline of the paper is as follows. Parameters of the channel are briefly described in section II. The measurement environment, the equipment and the methodology of subsequent *data acquisitions* are explained in detail in section III. The results of the estimated channel response, parameters of the channel and the effect of the spatial diversity are reported in section IV. Conclusions are drawn in section V.

## II. PARAMETERS OF THE MOBILE CHANNEL

### A. Channel model

Many physical factors in the radio propagation channel including multipath propagation, vehicle speed and surroundings objects, influence the received signal which may consist of a large number of attenuated, time delayed, phase shifted replicas of the transmitted signal. The random and complicated mobile radio channel can be modelled as a linear time variant filter [2]. The low-pass equivalent channel impulse response can be expressed as:

$$h(t, \tau) = \sum_{n=0}^{N(t)-1} A_n(t) e^{-j\theta_n(t)} \delta[t - \tau_n(t)] \quad (1)$$

where  $A_n(t)$  and  $\tau_n(t)$  are the amplitudes and the delays of the  $n$ th multipath component and  $N(t)$  is the number of paths.  $\theta_n(t)$  is the phase shift. Because of the motion of the vehicle and the surroundings objects, the parameters  $A_n(t)$ ,  $\tau_n(t)$ ,  $\theta_n(t)$  and  $N(t)$  are considered as randomly time-varying functions [3].

### B. Transfer function

The *time-varying* channel transfer function,  $H(f, t)$ , is calculated from the channel impulse response by applying the Fourier transform on the delay variable,  $\tau$ . The transfer function shows the channel bandwidth and the gain (or the fade) that the channel experiences to a frequency.

$$H(f, t) = F_{\tau} \{h(\tau; t)\} \quad (2)$$

### C. Scattering function

The scattering function  $S(\nu, \tau)$  provides the joint power distribution in the Doppler and delay domains. It represents the power spectral density with respect to Doppler frequency,  $\nu$ , and plotted in the delay domain,  $\tau$ . The scattering function is one of the eight system functions, defined by Bello

[4]. There is a duality between the Doppler frequency and the time variable  $t$ . To calculate the scattering function, we first compute the autocorrelation function of the time-varying channel impulse response,  $R_h(\tau, t)$ , and then apply the Fourier transform with respect to the time variable.

$$S(\tau, \nu) = F_{\Delta t}\{R_h(\tau, \Delta t)\} \quad (3)$$

If we do the integral on  $S(\tau, \nu)$  with respect to the delay variable, we obtain the power spectral density in Doppler shift domain.

$$P(\nu) = \int_0^\infty S(\tau, \nu) d\tau \quad (4)$$

If the maximum Doppler shift frequency  $\nu_{\max}$ , calculated from carrier frequency and mobile station velocity, is known, the power distribution with respect to the angle of arrival  $\varphi$  can be derived.

$$P(\varphi) \Leftrightarrow P(\nu) \quad \text{with } \varphi = \cos^{-1}(\nu/\nu_{\max}). \quad (5)$$

These functions give relevant spatial characteristics of the channel.

#### D. Power delay profile

The power delay profile, or the delay profile spectrum is determined as the mean power of the channel as function of the path delay  $\tau$  [2]. Individual power delay profiles,  $p_i(\tau)$ , can be computed from the square of the envelope of the low-pass impulse responses  $h_i(\tau)$ , where the index  $i$  indicates the  $i$ -th impulse response. The *Average Power Delay Profile* (APDP) over a set of  $M$  consecutive individual profiles is computed as [5]:

$$P(\tau_k) = \frac{1}{M} \sum_{i=1}^M p_i(\tau_k) \quad (6)$$

where  $k$  is the index of the delay samples of each profile. The square root of the second central moment of the power delay profile (the RMS delay spread) is defined as:

$$\sigma_\tau = \sqrt{\frac{\sum_{n=1}^N (\tau_n - \bar{\tau})^2 P(\tau_n)}{\sum_{n=1}^N P(\tau_n)}} \quad (7)$$

where  $\bar{\tau}$  is the average delay. From the RMS delay spread we can calculate the coherence bandwidth,  $B_c$ , which is a statistical measure of the range of frequencies over which the channel can be considered non selective or flat. The exact relationship between the coherence bandwidth and the RMS delay spread is a function of specific channel impulse responses. If the  $B_c$  is defined as the bandwidth over which the frequency correlation function is above 0.9, then we have [2]:  $B_c = 1/5\sigma_\tau$

#### E. Space diversity

The fundamental phenomenon of UHF radio propagation in the urban and suburban mobile radio environment is the existence of multipath with different and varying time delays. Different Doppler shifts are associated with scatter paths arriving at the vehicle from different angles. A common method to

improve the performance of wireless link is to use spatial diversity [7]. Diversity exploits the random of radio propagation by combining distinct paths into a stronger composite signal. The signals received from spatially separated antennas on the mobile may have ideally uncorrelated envelopes for antenna separations of one half wavelength or more. This condition is satisfied in our measurements.

Three types of combining methods are investigated to determine the performance improvement in signal statistics realized through space diversity, two-branch selection combining, equal gain combining and maximum ratio combining. If the received envelopes for the two branches are  $r_1(t)$  and  $r_2(t)$  respectively, then the resultant signal envelope,  $r_c(t)$  at the output of the combiner is given by [6]:

$$r_c(t) = \begin{cases} \max[r_1(t), r_2(t)] & \text{(selection combining)} \\ \frac{r_1(t) + r_2(t)}{\sqrt{2}} & \text{(equal gain combining)} \\ \sqrt{r_1^2(t) + r_2^2(t)} & \text{(maximal ratio combining)} \end{cases} \quad (8)$$

### III. EXPERIMENTAL PROCEDURE

#### A. Description of measurement locations

The measurement campaign planning was done according to the objective of characterizing the digital terrestrial television propagation channel for mobile applications by means of an analysis of the time and spatial received signal in different environments. The DTV station, covering Ottawa and the surroundings, is located at Manotick, about 30 km south of Ottawa. Figure 1 shows the different environments where the receiver vehicle travelled:

- In the suburban area, i.e. *site 1*, collected 16 data records were collected. This location consists of single two storey houses with some trees and is located about 10 km from the ATSC DTV transmitter. The vehicle travelled each street in the opposite directions at a speed of 30 km/h.
- 16 data were recorded from the rural area, *site 2*, which is about 9 km from the DTV station. There were no obstructions and the vehicle was travelling at 40 km/h, 50 km/h and 60 km/h.
- *Site 3* represents a urban area. It was located downtown Ottawa (Somerset street) with no obstructions from high-rise buildings. 2 data files were recorded from this urban area where the van speed was 30 km/h and about 25 km from the transmitter.
- *Site 4* and *site 5* represent highway environments (i.e. Highway 417 (East-West orientation) and Highway 416 (North-South orientation) respectively. These locations were located at 24, 16 and 15 km from the DTV station and the vehicle speed was about 100 km/h. 6 data files were recorded in highway conditions.

#### B. Measurement technique

The measurement signal was transmitted from an omnidirectional antenna at a height of 215.4 m above ground with

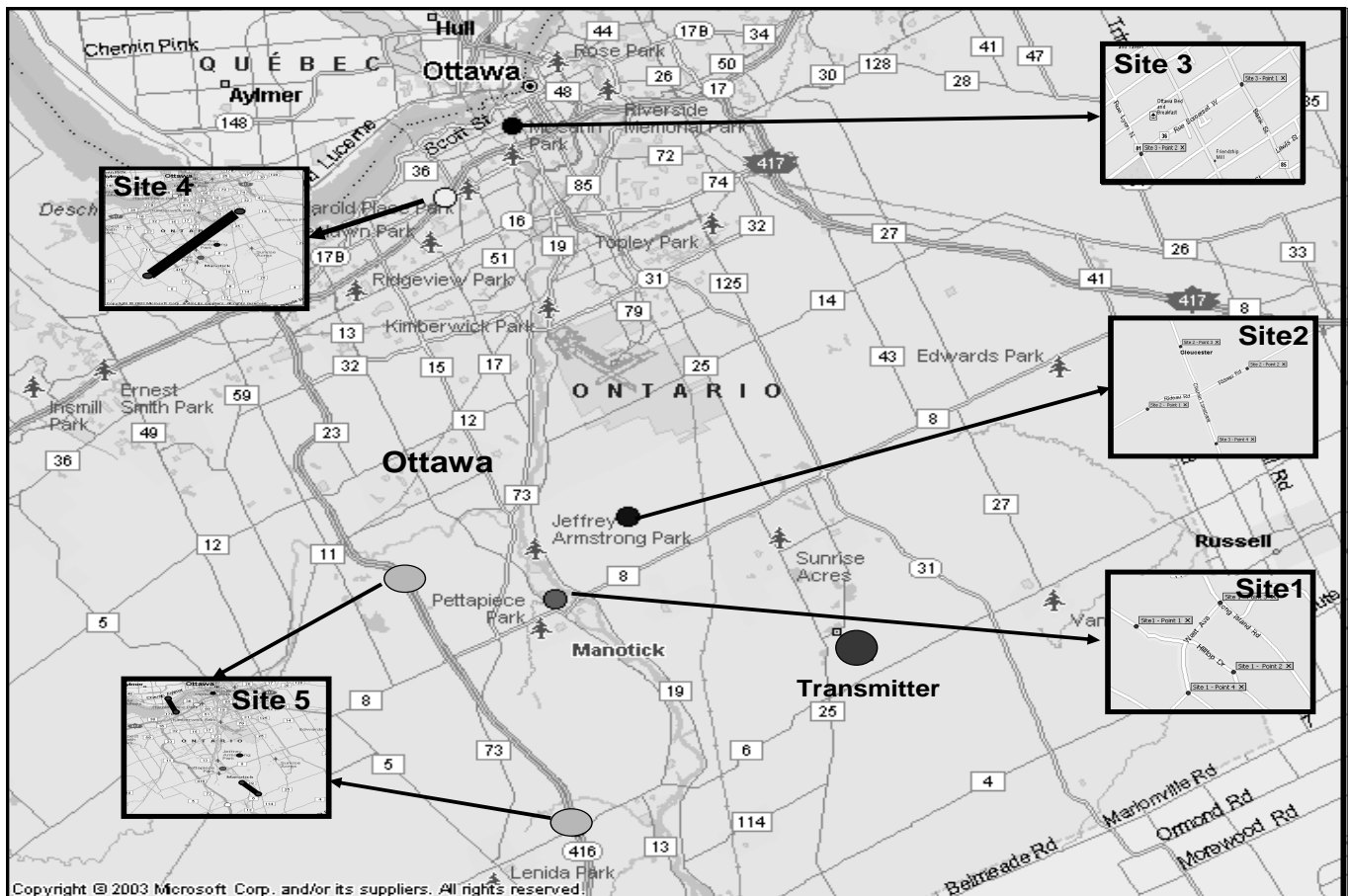


Fig. 1. Measurements locations of the DTV transmitter and different sites in Manotick (near Ottawa), for urban, suburban, rural and highway transmission environments.

30 kW ERP on UHF channel 67 channel (788-794 MHz) [8]. The digital terrestrial system transmits a 19.39 Mbps serial data stream comprised of 188-byte MPEG-2 data packets. Data randomization, Reed-Solomon channel coding, interleaving and trellis coding are used to provide error protection. The ATSC standard uses an eight-level Vestigial Sideband (8-VSB) modulation scheme with a pilot signal. The randomized data and coded packets are formatted into data frames and data fields. Each data field is divided into 313 segments and begins with one complete Data Field Sync which contains a pseudo-random sequence PN-511 [1]. This sequence is used as a training signal for the receiver's equalizer and is used here to estimate the channel impulse response. The channel RF bandwidth is 6 MHz. The receiver, figure 2, is installed in a mobile vehicle and connected to two omni-directional antennas located on the roof. The two antennas with 6-wavelength separation, have identical radiation patterns and polarizations. The 8-VSB signal is received using a professional DTV tuner which brings the signal down to an IF of about 43-47 MHz. The tuner output is downconverted to a lower IF of 5.38 MHz, comparable to the VSB symbol rate, filtered and then the envelope of the received signal from each branch is stored on digital tape for computer processing. The mobile

measurements have been made in order to record as much received samples as possible along a route with different vehicle speeds. The duration of each recorded data file is 42 seconds.

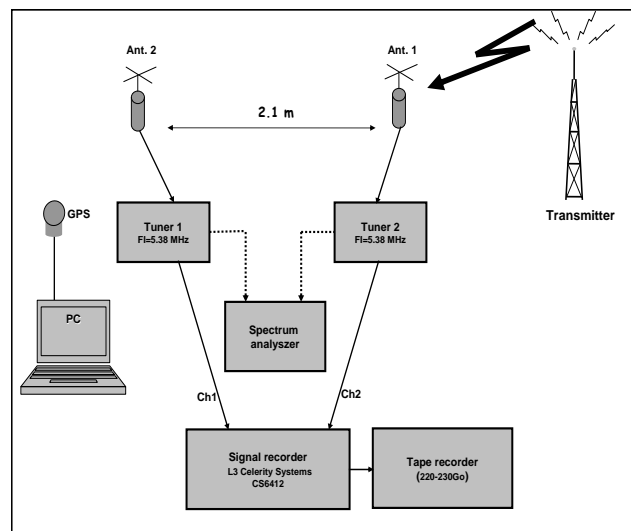


Fig. 2. Simplified block diagram of the measurement equipment.

#### IV. Experimental measurements

In this section, the statistical channel parameters obtained from the experimental measurements are presented.

##### A. Channel impulse responses

Channel estimation relies entirely on the ATSC data-field sync segments, described in [1], and particularly on the 511-PN (pseudo-noise) sequences. The data-field sync segment is transmitted once every 24.2 ms approximately whereas the time duration of the PN sequence is only 47.48  $\mu$ s. This part of recorded data is used for channel estimation. For each recorded data, after downconverting the received signal to a 5.38 MHz IF frequency, we locate the (time) position of the first 511-PN sequence. Then the received signal is passed through an IF noise and interference limiting filter. The channel response is obtained by correlating the baseband filtered signal with a reference signal based on the PN sequence. This approach to estimate the channel response is similar to the sliding correlator technique [2] except that the PN sequence is embedded in the DTV signal.

Figure 3 illustrates the spatial fluctuations of the impulse responses observed at antenna 1, in a urban area with vehicle speed of about 30 km/h, in a suburban area at 30 km/h as well, in a rural area with a receiver speed of 60 km/h, and on Highway 416 where the mobile travels at 100 km/h. The impulse responses are obtained from 40 successive frames, corresponding approximately to mobile path lengths of 8 m (urban and suburban areas), 16 m (rural area), and 26 m (highway). This figure shows how the channel behavior changes in different areas. The direct path between the DTV transmitter and the mobile antenna is often blocked. Multipath components contributing to the impulse responses originate from reflections and diffractions of direct waves at the surrounding structures, resulting in a strong attenuation of the dominant component. However, for the highway recording, one can see that the amplitude of the received signal is almost constant compared to the other areas especially the suburban and urban areas where the amplitude fluctuations of the dominant component is more pronounced.

##### B. Transfer functions

Figure 4 shows the *average* transfer function magnitude from the same four recordings (urban, suburban, rural and highway). From this figure, one can observe that they are wide-band frequency selective channels with amplitude fluctuations in the [0, 30 dB] range.

##### C. Scattering functions and power angular spectra

Figure 5 shows the scattering functions for the four measured channels. For the urban channel, the received power, measured at the antenna 1, concentrates in the Doppler frequency range between 13 and 20 Hz and in the delay range of 0.3 to 0.6  $\mu$ s.

Figure 6 shows the angle of arrival (AoA) distribution corresponding to the four previously mentioned measurements. With the urban channel, most of signals arrived at antenna 1

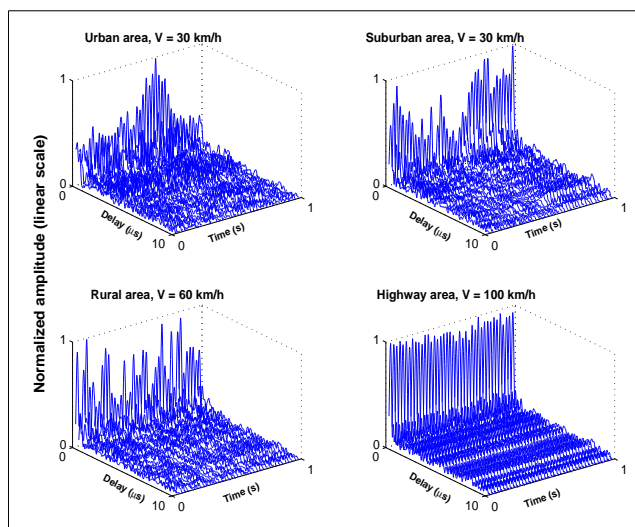


Fig. 3. Typical spatial fluctuations of the impulse response over 40 successive frames for urban, suburban, rural, and highway areas (files: *downtown\_040108\_site3*, *040107\_site1a*, *040107\_site2a*, and *416\_040226\_1*).

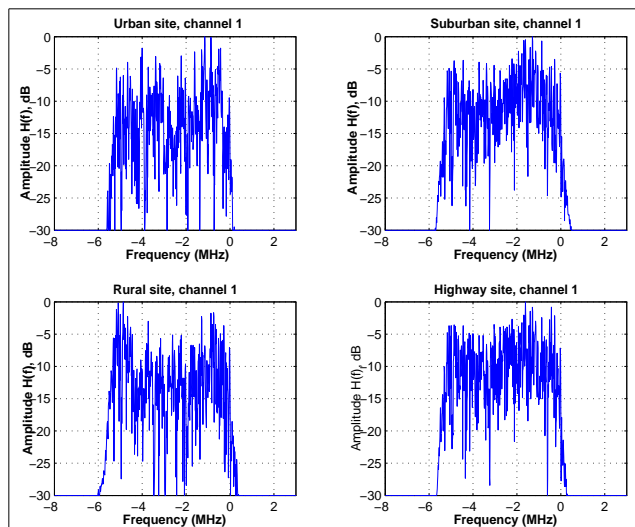


Fig. 4. Transfer functions amplitude for urban, suburban, rural, and highway areas (files: *downtown\_040108\_site3*, *040107\_site1a*, *040107\_site2a*, and *416\_040226\_1*).

from a direction of 40°. Measurement at channel 2 (figure 7) shows a similar performance: most of signals arrived from 30°.

The scattering function of the suburban channel shows that the signal power is concentrated within three directions with Doppler frequency intervals [21, 17] Hz, [14, -4] Hz and [-17, -22] Hz. From the corresponding power angular spectra, we note that most of the signal energy comes from the [20°, 50°] and [50°, 100°] angle of arrival ranges.

The scattering function and the power angular spectrum of the rural channel recordings show that most of the power is concentrated in the Doppler frequency intervals [3, 10] Hz

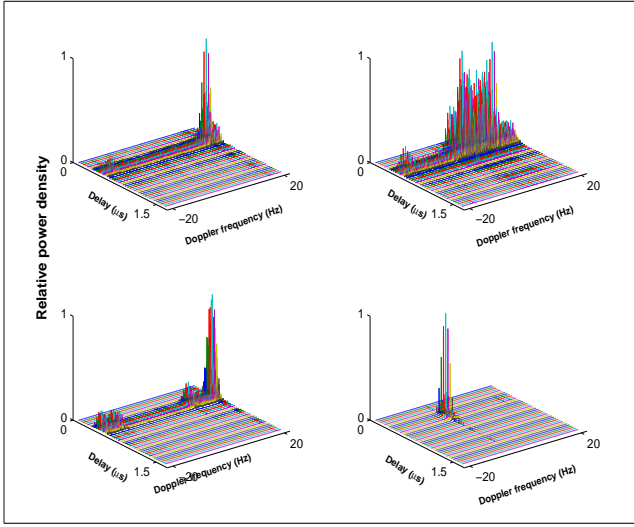


Fig. 5. Scattering functions for urban, suburban, rural, and highway areas (files: *downtown\_040108\_site3*, *040107\_site1a*, *040107\_site2a*, and *416\_040226\_1*).

and corresponding angle of arrivals  $[77^\circ, 87^\circ]$ , as well as  $[21, 17]$  Hz Doppler range (i.e.  $[62^\circ, 67^\circ]$  angle of arrivals). For these measurements, the arrival angular dispersion is narrower than that observed for the urban and the sub-urban channels. From figure 6, one can see that lower power signal components arrive from other directions: i.e.  $[67^\circ, 75^\circ]$ ,  $[110^\circ, 118^\circ]$  and  $[140^\circ, 170^\circ]$ .

For the highway channel measurements, the power angular spectra show that most of the signals is received with an angle of arrival of  $93^\circ$ , that is, nearly perpendicular to the moving direction of the van. This results in a low Doppler shift in this case. We made the same observation with antenna 2. In figure 7, the angle of arrival of the highway channel observed at antenna 2 is concentrated around  $92^\circ$ .

Evaluating the Doppler spectra is possible if the sampling theorem in space is satisfied, i.e.:  $\Delta t \leq 1/2f_{dmax}$ , where  $\Delta t$  is the time difference between two successive impulse responses and  $f_{dmax}$  is the maximum Doppler frequency. For the ATSC 8-VSB system, the pseudo-random sequence PN-511 is transmitted once every 24.2 ms approximately: therefore the speed of the measuring vehicle have to be smaller to 28 km/h. This condition was not satisfied in our measurements. This is why, for the power density spectra, one can only observe the signals within the  $[-20.7, 20.7]$  Hz Doppler frequency range. Due to the sampling rate limitation, the distribution of angle of arrival can be observed only in the intervals between:

- $[18^\circ, 162^\circ]$  for urban and suburban areas, where the maximum Doppler frequency is 22 Hz,
- $[62^\circ, 118^\circ]$  for rural areas where the maximum Doppler frequency is 44 Hz,
- and  $[73^\circ, 107^\circ]$  for highway conditions where the maximum Doppler frequency is 74 Hz.

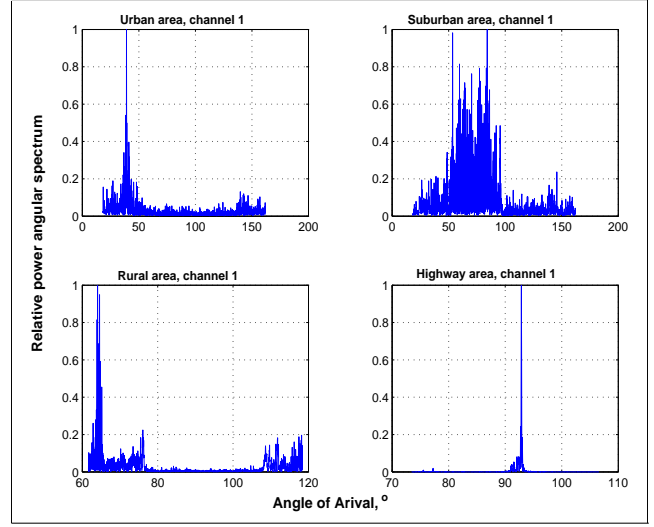


Fig. 6. Angle of arrival distribution for urban, suburban, rural, and highway areas (files: *downtown\_040108\_site3*, *040107\_site1a*, *040107\_site2a*, and *416\_040226\_1*), channel 1.

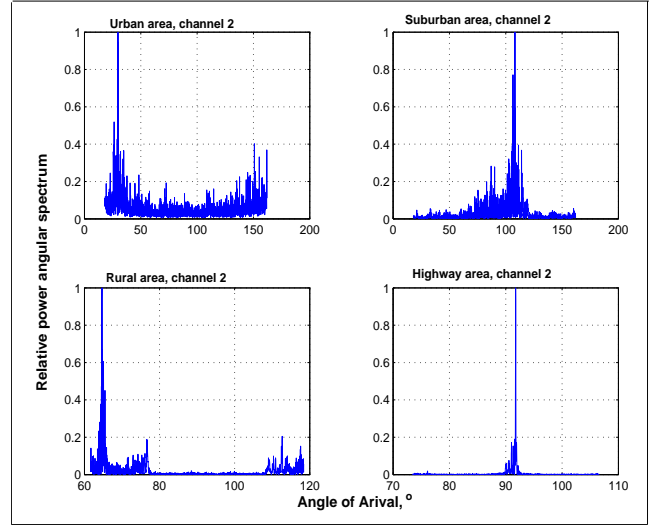


Fig. 7. Angle of arrival distribution for urban, suburban, rural, and highway areas (files: *downtown\_040108\_site3*, *040107\_site1a*, *040107\_site2a*, and *416\_040226\_1*), channel 2.

#### D. Power delay profile

An average power delay profile was determined from 10 successive power delay profiles according to the following procedure:

- step 1: the total power for each power delay profile was calculated;
- step 2: the greatest total power from each 10 consecutive power delay profiles was identified, i.e.  $P_{max}$ ;
- step 3: any of the ten power delay profiles with a total power 10 dB or more below  $P_{max}$  was considered invalid and excluded from the processing;
- step 4: a set of valid power delay profiles within the succession of 10 power delay profiles were averaged to

give an average power delay profile.

To ensure that the noise contribution is negligible in the statistical computations, only relevant multipath components are taken into account. The thresholds were chosen as proposed in ITU recommendation ITU-R P.1407-1 [9]: i.e. 12dB, and 15dB. The signal level below the threshold value was set to zero and was not counted in the statistics.

Figure 8 depicts the average power delay profiles from the same areas considered in the last section. For those values of the RMS delay and the average delay indicated in the graphics, the threshold was 15 dB. Examination of these figures indicates the existence of many multipath components in the suburban and urban areas which fade with relative level 1 dB and more below the dominant component. In the downtown area, which represents a urban environment, the first multipath component have a power level as large as the dominant component, and is typical of worst case conditions for a mobile operating in an environment which contains several scattering obstructions. In such areas, the measurements show additional strong peaks with longer delays, typically paths with delays up to  $10\mu s$ . One can clearly see three peaks with relative level 10 dB below the first path. The average power delay profiles from the urban area exhibit an RMS delay twice as large as the RMS delay from the suburban area. The measurement from the highway and the rural environments show one multipath with relative level between 15 dB and 10 dB below the first component. For suburban, rural and highway environments, the multipath components are concentrated within a delay window of about 1-2  $\mu s$ . From the highway and rural areas, the RMS delay are less than 0.1  $\mu s$ .

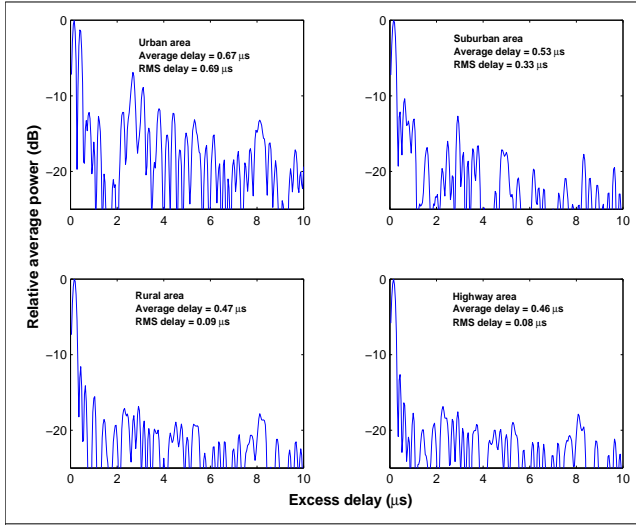


Fig. 8. Average power delay profiles for urban, suburban, rural, and highway environments. The RMS delay spread and the average delay are computed using a 15 dB threshold (files: *downtown\_040108\_site3*, *040107\_site1a*, *040107\_site2a*, and *416\_040226\_1*).

Figure 9 shows the cumulative distributions of the RMS delay spread for urban, suburban, rural and highway areas using a 15 dB threshold in each power delay profile. Comparing

the cumulative distributions from channel 1 and channel 2, one observes that the probability of exceeding the RMS delay spread is higher for urban area measurements than for the other environments. This suggests that there are more multipath present in the urban measurements (downtown) than in the suburban, rural and highway sites. For instance, for channel 2, the probability of exceeding an RMS delay spread of  $2\mu s$  is about 0.7 for the urban site, 0.3 for the suburban site and only 0.02 for the rural and highway sites. The curves indicate that for each area, one channel has lower RMS delay spread values than the other. This result is not pronounced in the urban area where the probability to exceed an RMS value is slightly different.

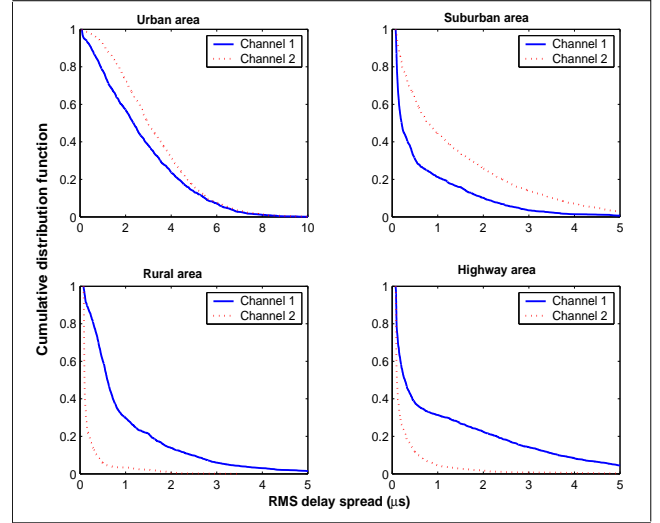


Fig. 9. Cumulative distributions of the RMS delay spread for urban, suburban, rural and highway areas using a 15 dB threshold for each power delay profile.

Table I gives the RMS delay for the total average power delay profile of each area, the coherence bandwidth  $B_c$  calculated as defined in section II. The Doppler spread is equal to the maximum frequency Doppler  $f_m$  and the coherence time  $T_c = \sqrt{9/16\pi f_m^2}$  [2]. Those values are obtained from the same recordings described in the last sections. Based on the multipath delay spread and the Doppler spread values, the channel can be classified as frequency selective and slow fading channel.

| Data     | $\sigma_\tau$ ( $\mu s$ ) | $B_c$ (kHz) | $B_D$ (Hz) | $T_c$ (ms) |
|----------|---------------------------|-------------|------------|------------|
| Rural    | 1.2458                    | 160         | 22         | 19.2       |
| Suburban | 0.1494                    | 1338        | 22         | 19.2       |
| Rural    | 0.0978                    | 2045        | 44         | 9.6        |
| Highway  | 0.2161                    | 925         | 74         | 5.7        |

TABLE I  
CHANNEL PARAMETERS

### E. Space diversity

Due to the rapidly changing character of the multipath process, the local mean from the received signals is subtracted

from the signal before the computation of the resultant signal output of the combiner. Five signals are superposed in figure 10, two of them corresponds to the actual signals received by the two antennas while the others result from the combining techniques. This figure shows the (ideal) diversity results for the measured signal in a suburban area, located at 9 km from the transmitter, and for which the vehicle speed is about 30 km/h. As given in 8, selection diversity chooses the strongest signal, while equal gain combines the cophased signal voltages with equal weights, and maximal ratio weights the cophased signal by itself, equivalent to a sum of the signal powers. Note that the maximal ratio combining should weight signal voltages according to their relative signal to noise ratio; however, as the noise may not be known a priori, signal strength alone is used here. As expected, the diversity gain achieved by the maximum ratio combiner is higher than that for the equal-gain combining and the selection combining techniques.

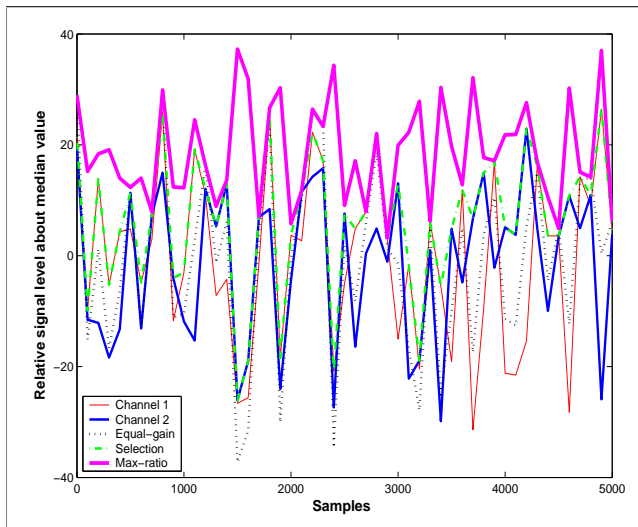


Fig. 10. Relative amplitude of the received signal about the median value from each antenna and resultant envelope (ideal combining scenario) for the three combining methods (file: *FieldTest\_030714\_A12*).

Figure 11 shows the relative envelope signal received from each antenna and the resultant signal from the maximum-ratio combining for the same data as presented in the last sections. Figure 11 indicates that, as the fading does not occur at the same time from one antenna to the other, the fade contributions are significantly mitigated by the combination process.

## V. CONCLUDING REMARKS

The measurements presented in this paper show the channel characteristics of 4 different types of propagation environments. The channel impulse response and the power delay profile show the characteristics of the multipath components: the number of multipath components and their power distribution. There are more multipath components in the urban and the suburban channels than in the rural and the highway channels. The transfer functions show that the channel is wideband and

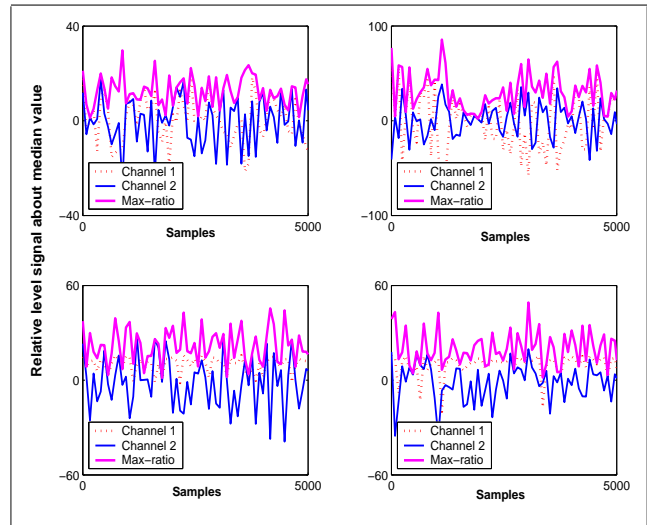


Fig. 11. Relative amplitude of the received signal about the median value from each antenna and the resulting envelope with maximum-ratio combining (files: *downtown\_040108\_site3*, *040107\_site1a*, *040107\_site2a*, *417\_040108\_site4*).

frequency-selective within the ATSC signal bandwidth. The scattering functions show the joint distribution of power in Doppler frequency and delay domains: this provides insight about the distribution of the surrounding scatterers of each channel. The power angular spectrum shows the distribution of the direction of arrival of the multipath components, relatively to the mobile direction. The urban and the sub-urban channels have a wider signal arrival angle spreads than the rural and the highway channels. For the highway channels, there is a line of sight component and the arrival signal rays concentrate around this direction. Furthermore, our measurements also shows that the sampling frequency of the impulse response is too low relative to the channel coherence time. Also, the channel characteristics obtained from our measurements may suggest some relevant design considerations in order to exploit ATSC signals in mobile wireless scenarios. Space diversity is deemed necessary to insure proper performance in mobile conditions.

## Acknowledgments

The authors are greatly indebted to Mr. Bernard Caron, Mr. Robert Gagnon and Mr. Benoit Ledoux from the Television Broadcast Technologies Research Group at the Communication Research Centre in Ottawa, who very kindly provided the channel measurement facilities essential to this work. The authors would also like to thank Mr. Sili Lu for his help in the preparation of this paper.

## REFERENCES

- [1] ATSC, *ATSC Digital Television Standard*, ATSC standard A/53, september 1995.
- [2] T. S. Rappaport, *Wireless communications*, Prentice-Hill, Inc, 2002.
- [3] S. Parsons, *The mobile radio propagation channel*, Pentech Press, London, 1992.
- [4] P. A. Bello "Characterization of randomly timevariant linear channels", *IEEE Trans. Comm. Syst.*, Bd. CS-11, No. 4, pp. 360-393, 1963.

- [5] D. Cox, *Delay doppler characteristics of multipath propagation at 910 MHz in a suburban mobile radio environment*, IEEE Trans. on Ant. and Propagation, VOL. AP-20, No. 5, pp. 625-635, september 1972.
- [6] A. M. D. Turkmani, A. A. Arowojolu, P. A. Jefford and C. J. Kellett *"An experimental evaluation of the performance of two-branch space and polarization diversity schemes at 1800 MHz"*, IEEE Trans. on Veh. Tech., vol. 44, No. 2, pp. 318-326, may 1995.
- [7] W. C. Jakes, *"A comparison of specific space diversity techniques for reduction of fast fading in UHF mobile radio systems"*, IEEE Trans. on Veh. Tech., vol. VT-20, No. 4, pp. 81-93, nov. 1971.
- [8] Y. Wu, X. Wang, K. Salehian, H. Jun and B. Caron *Recent performance improvements to the ATSC transmission system*, International Broadcasting Convention, Amsterdam, pp. 123-133, september 2003.
- [9] ITU-R Rec. P. 1407-1, *"Multipath propagation and parameterization of its characteristics"*, 1999-2003.